Universiteit
Leiden
The Netherlands

Chemical genetic approaches for target validation

Wel, T. van der

Citation
Wel, T. van der. (2020, January 22). *Chemical genetic approaches for target validation*. Retrieved from https://hdl.handle.net/1887/83257

Version:	Publisher's Version
License:	Licence agreement concerning inclusion of doctoral thesis in the Institutional Repository of the University of Leiden
Downloaded from:	https://hdl.handle.net/1887/83257

Note: To cite this publication please use the final published version (if applicable).

Cover Page

Universiteit Leiden

The handle http://hdl.handle.net/1887/83257 holds various files of this Leiden University dissertation.

Author: Wel, T. van der
Title: Chemical genetic approaches for target validation
Issue Date: 2020-01-22

3

Precise gene editing allows visualization of endogenous FES kinase engagement during myeloid differentiation

Introduction

A single human cell may contain over 100 different kinases that work together in a highly regulated network with various physiological functions.[1,2] Overexpression of a kinase to study its role may therefore disturb the intrinsic balance of the kinase signaling network, leading to compensatory changes and other artefacts in cellular processes.[3] This is particularly troublesome in validation of kinases as therapeutic target, as inactivation of overexpressed (and sometimes constitutively active) kinases using small-molecule inhibitors may not match the functional effects resulting from inhibition of endogenously expressed kinases with tightly regulated activity. A prominent example was already observed in chapter 2 (Figure 2.6E), where overexpression of FES kinase in U2OS cells drastically altered the global cellular phosphotyrosine profile.

Endogenous FES expression levels are highest in cells of hematopoietic origin, especially those in the myeloid lineage, but FES is also expressed in neuronal, endothelial and epithelial cells.[4] Its initial discovery in terminally differentiated myeloid cells led to multiple studies examining its function in myeloid differentiation. For instance, stable overexpression of FES in K562 cells or transient overexpression of constitutively active FES in U937 cells induces myeloid differentiation towards macrophages.[5,6] In addition, antisense-mediated knockdown of FES in HL-60 cells was reported to block macrophage differentiation induced by phorbol 12-myristate 13-acetate (PMA).[7] Deletion of FES in transgenic mice (*fes*$^{-/-}$) resulted in decreased numbers of B lymphocytes and increased numbers of monocytes and neutrophils[8], although these effects were not observed in a second, independently generated *fes*$^{-/-}$ mouse strain.[9] This latter study is in line with the observation that genetic knockout of FES in mouse embryonic stem cells (ESCs) does not impair differentiation towards macrophages, nor towards any other tested myeloid cell type.[8] Follow-up studies employing transgenic mice expressing a kinase-dead FES variant (*fes*^{KD}) also reported no hematopoietic defects. In contrast, mice expressing an artificial, myristoylated variant (*fes*^{MF}) that harbors constitutive membrane association and thereby increased kinase activity, display increased levels of circulating myeloid cells and decreased levels of erythrocytes and platelets.[10]

Taken together, these observations indicate that FES activity is likely to be tightly regulated and that overexpression or constitutive activation of FES disrupts this regulatory process and thus conceals the true physiological role of FES. It remains unclear to what extent congenital, long-term disruption of FES activity in knockout animals induces compensatory mechanisms, such as upregulation of FER. Moreover, the question rises whether the observed effects are dependent on the scaffold function of FES, *e.g.* membrane localization via its F-BAR domain, or on its kinase activity. Here, the chemical genetic toolbox as described in chapter 2, encompassing the use of engineered FES^{S700C} in combination with covalent, complementary probes, is applied to

pharmacologically modulate endogenous FES activity and study its role during myeloid differentiation.

Results

Gene editing allows visualization of kinases by complementary probes in human cells

To obtain a physiologically relevant model system and avoid the use of transient overexpression, CRISPR/Cas9 gene editing was employed to introduce the S700C mutation endogenously in the human HL-60 promyeloblast cell line (Figure 3.1A and 3.1B, step 1-2). Endogenous FES^{S700C} and its engagement by inhibitors can next be visualized using the mutant-specific probes WEL028 and WEL033 and covalently bound targets can be identified using quantitative label-free chemical proteomics (Figure 3.1B, step 3). Wild-type and mutant cells share potential off-targets of WEL028 with the sole exception of FES, which is exclusively targeted in mutant cells. This feature allows for a comparative experimental setup, which is instrumental to dissect on-target from off-target effects and gain insight in the role of FES activity in myeloid differentiation (Figure 3.1B, step 4).

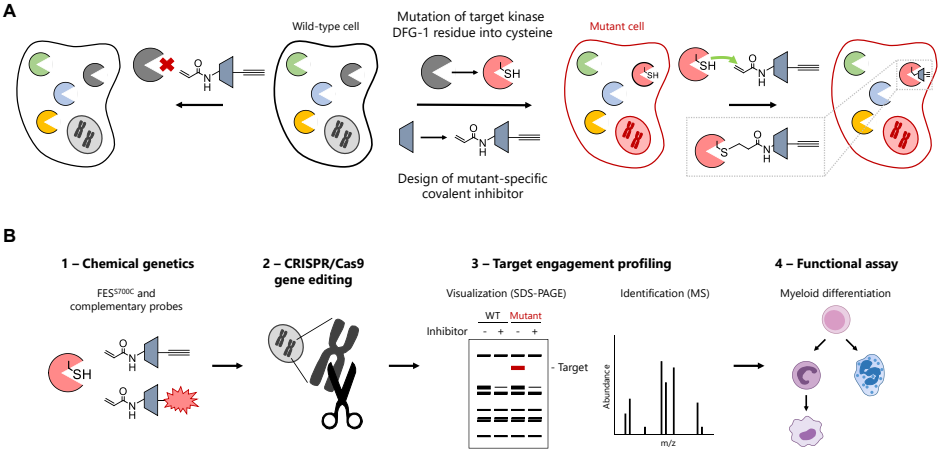

Figure 3.1 – Chemical genetic strategy and workflow to visualize endogenous kinase activity and target engagement. (A) General strategy involving mutagenesis of a kinase DFG-1 residue in a cell line using CRISPR/Cas9 gene editing. This circumvents the use of overexpression that may disturb balanced endogenous signaling networks. Wild-type cells function as control cells to account for potential off-targets of the covalent inhibitor. **(B)** Schematic workflow encompassing the application of chemical genetic tools described in chapter 2 in an endogenous model system, generated with the use of CRISPR/Cas9 gene editing. Endogenous mutant FES can subsequently be visualized using mutant-specific complementary probes and probe targets can be identified using quantitative label-free proteomics and mass spectrometry analysis. Using this strategy, the role of FES activity during myeloid differentiation can be studied.

HL-60 cells are a widely used model system for myeloid differentiation, since they are capable to undergo differentiation along the neutrophil as well as monocyte/macrophage lineage, depending on the differentiation agent (Figure 3.2A).[11,12] To sensitize endogenously expressed FES in HL-60 cells to the mutant-specific probe, a single guide (sg)RNA target was selected with predicted site of cleavage in close proximity of the desired mutation in exon 16 of the human genomic *FES* locus (Figure 3.2B). In conjunction, a single-stranded oligodeoxynucleotide (ssODN) homology-directed repair (HDR) donor template was designed, aimed to introduce the target S700C mutation along with the implementation of a restriction enzyme recognition site to facilitate genotyping using a restriction fragment length polymorphism (RFLP) assay. Of note, the ssODN donor also included silent mutations to prevent cleavage of the ssODN itself or recleavage of the genomic locus after successful HDR (Figure 3.2B). HL-60 cells were nucleofected with plasmid encoding sgRNA and Cas9 nuclease along with the ssODN donor, followed by single cell dilution to obtain clonal cultures. Screening of clones using the RFLP assay led to the identification of a homozygous S700C mutant clone (Figure 3.2C). Sanger sequencing verified that the mutations had been successfully introduced without occurrence of undesired deletions or insertions (Figure 3.2D). No off-target cleavage activity was found in predicted putative off-target sites (Supplementary Figure 3.1 and Supplementary Table 3.1).

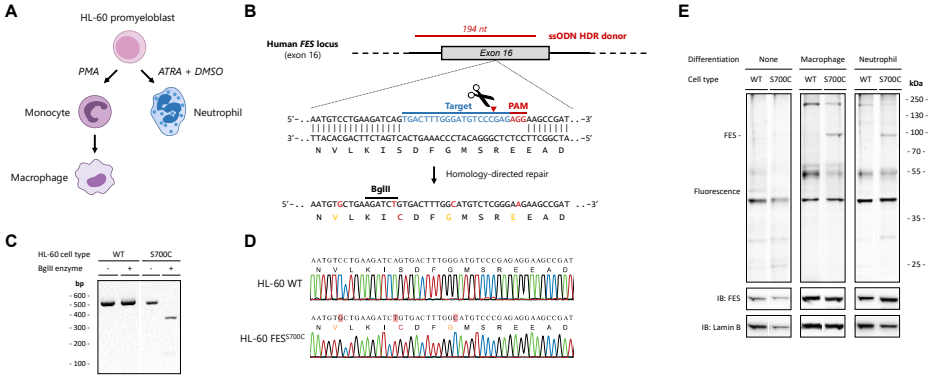

Figure 3.2 - Visualization of endogenous FES^{S700C} in CRISPR/Cas9-edited HL-60 cells. (A) HL-60 cells can differentiate into macrophages upon stimulation with PMA or into neutrophils with all-trans-retinoic acid (ATRA) and DMSO. **(B)** CRISPR/Cas9 gene editing strategy for introduction of S700C point mutation in the genomic *FES* locus. Selected sgRNA (bold blue) directs Cas9 to cleave at predicted site (red triangle). A ssODN homology-directed repair (HDR) donor template (red) flanks introduced mutations with 80 bp homology arms. The S700C mutation generates a BglII restriction site along with three silent mutations (orange) to remove PAM sites. Of note, two of the three mutated PAM sites correspond to sgRNAs not used in this study. PAM: protospacer-adjacent motif. **(C)** Restriction-fragment length polymorphism (RFLP) assay for identification of HL-60 FES^{S700C} clone. Genomic region was amplified by PCR and amplicons were digested with BglII. Expected fragment size after digestion: 365 + 133 bp. **(D)** Sequencing traces of WT HL-60 cells and homozygous FES^{S700C} HL-60 clone. No deletions, insertions or undesired mutations were detected. **(E)** Endogenous FES is visualized by WEL033 in differentiated HL-60 FES^{S700C} cells. Wild-type or FES^{S700C} HL-60 cells promyeloblasts, macrophages or neutrophils were lysed, followed by labeling with WEL033 (1 µM, 30 min, rt). FES expression increases upon differentiation (anti-FES immunoblot).

Next, wild-type and HL-60 FES^{S700C} cells were differentiated into macrophages or neutrophils and the corresponding cell lysates were incubated with fluorescent probe WEL033 to visualize endogenous FES (Figure 3.2E). In-gel fluorescence scanning of the WEL033-labeled proteome of differentiated FES^{S700C} HL-60 cells revealed a band at the expected MW of FES (~93 kDa), which was absent in wild-type HL-60 cells. Furthermore, the fluorescent band was less prominent in non-differentiated HL-60 FES^{S700C} cells, probably due to lower FES expression levels prior to differentiation (Figure 3.2E, anti-FES immunoblot). Of note, WEL033 labeled a number of additional proteins (MW of ~200, ~55 and ~40 kDa, respectively) at the concentration used for FES detection (1 μM). In short, these results demonstrate that endogenously expressed engineered FES can be visualized using complementary chemical probes.

Pharmacological inactivation of FES activity during myeloid differentiation

FES was previously reported as an essential component of the cellular signaling pathways involved in myeloid differentiation.[7,13] However, most of these studies relied on the use of overexpression, constitutively active mutants, or antisense-based knockdown of FES. In addition, it remains unclear whether this role of FES is dependent on its scaffold function or kinase activity. To investigate whether acute pharmacological inactivation of endogenous FES activity affected myeloid differentiation, living wild-type and FES^{S700C} HL-60 cells were incubated with WEL028 (100 nM or 1 μM) during PMA-induced differentiation towards monocytes/macrophages. To ensure complete FES inhibition at the moment of differentiation initiation, cells were pretreated with WEL028 2 h prior to addition of PMA. The growth medium was refreshed after 24 h to maintain FES inhibition, since recovery of active FES upon prolonged (> 48 h) exposure to WEL028 was observed, possibly due to protein resynthesis. Cells were harvested and lysed, followed by labeling of residual active FES^{S700C} by WEL033 (Figure 3.3A). This revealed full target engagement of engineered FES at a concentration of 100 nM WEL028 (Figure 3.3B), with only one identified off-target (~200 kDa). At the higher concentration of 1 μM, WEL028 was less selective and also inhibited additional WEL033-labeled targets.

The percentage of differentiated cells after treatment with the differentiation agent was quantified by monitoring surface expression of CD11b, a receptor present on HL-60 macrophages but not on non-differentiated HL-60 cells.[14] Strikingly, despite complete inhibition of FES^{S700C} at 100 nM WEL028 (Figure 3.3B), the percentage of CD11b-positive cells was unaltered (Figure 3.3C, D). Cell proliferation, an indirect hallmark of differentiation, was decreased to identical levels for FES^{S700C} HL-60 cells treated with vehicle or 100 nM WEL028 (Figure 3.3E). Accordingly, FES^{S700C} HL-60 cells treated with 100 nM WEL028 acquired macrophage morphology (*e.g.* adherence to plastic surfaces, cell clumping and cellular elongation) comparable to vehicle-treated controls (Figure

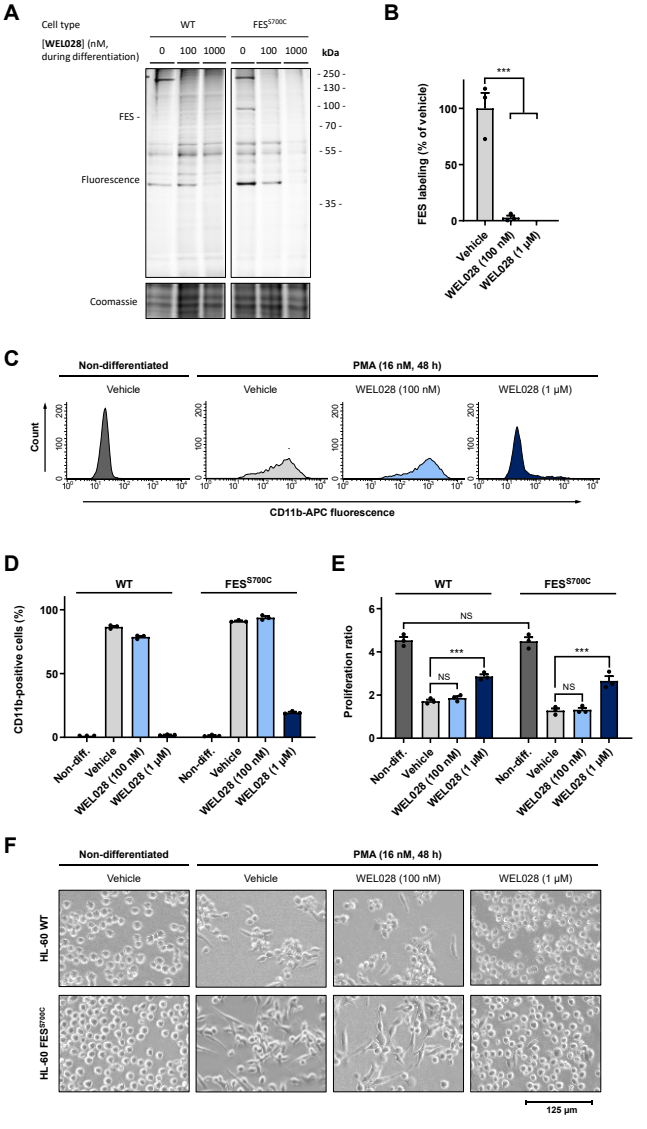

Figure 3.3 – FES activity is dispensable for differentiation of HL-60 cells into macrophages. (A, B) Target engagement profile of WEL028 on WT and FES^{S700C} HL-60 cells treated during PMA-induced differentiation. Cells were pretreated with vehicle or WEL028 (100 or 1000 nM, 1 h) prior to induction of differentiation towards monocytes/macrophages with PMA (16 nM, 48 h). Medium was refreshed with growth medium containing WEL028 and PMA after 24 h to maintain full FES inhibition. Lysates were incubated with WEL033 (1 µM, 30 min, rt). Band intensities were normalized to vehicle-treated control. **(C, D)** CD11b surface expression analyzed by flow cytometry. Threshold for CD11b-positive cells was determined using isotype control antibody. Histograms illustrate representative replicates of FES^{S700C} cells. **(E)** Proliferation of WT and FES^{S700C} HL-60 cells subjected to PMA-induced differentiation. Proliferation ratio: live cell number after differentiation divided by live cell number before differentiation. **(F)** Morphological inspection of WT and FES^{S700C} HL-60 cells. Shown images are representative for multiple acquired images at 20x magnification from replicates. All data represent means ± SEM (N = 3). Statistical analysis was performed using ANOVA with Holm-Sidak's multiple comparisons correction, *** P <0.001; NS if P >0.05.

3.3F). Together, these results show that complete FES inhibition does not affect PMA-induced differentiation of HL-60 cells into macrophages, suggesting that FES activity is dispensable for this process.

Remarkably, FES^{S700C} cells undergoing PMA-induced differentiation in presence of a higher concentration of WEL028 (1 µM) completely failed to express CD11b, exhibited a less pronounced decrease in proliferation and displayed phenotypic characteristics similar to non-differentiated cells (Figure 3.3C-F). Competitive probe labeling experiments revealed that WEL028 targets multiple off-targets at a concentration of 1 µM (Figure 3.3A), which suggested that the observed block in differentiation might be due to off-targets. A beneficial feature of the used chemical genetic strategy is that wild-type cells can be included to account for these off-targets. Indeed, 1 µM WEL028 had similar effects on CD11b surface expression, proliferation and morphology of wild-type HL-60 cells subjected to differentiation (Figure 3.3D-F). This verifies that the functional effects of WEL028 at 1 µM can indeed be attributed to off-target rather than on-target effects.

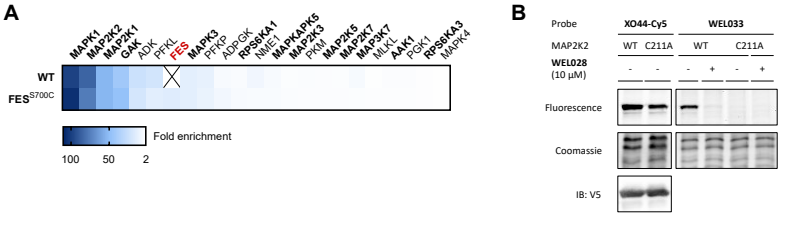

Figure 3.4 – Cellular selectivity profile of WEL028. (A) Chemical proteomic analysis of WEL028 kinase targets at 1 µM. WEL028-labeled proteome (1 µM, maintained for 48 h during differentiation) was conjugated to biotin-azide using click chemistry (2 eq., 1 h, 37 °C), followed by chemical proteomics workflow. Kinases with >2-fold enrichment compared to vehicle control were designated as targets. Kinases with native cysteine at DFG-1 position are shown in bold. Values represent means of fold enrichment (N = 3). Statistical analysis was performed using *t*-test with Benjamini-Hochberg multiple comparison correction, FDR = 10%. **(B)** Validation of MAP2K2 as off-target of WEL033 via covalent addition to DFG-1 residue Cys211. Recombinantly expressed MAP2K2 (wild-type or C221A mutant) in U2OS cell lysate was pre-incubated with WEL028 (10 µM, 30 min, rt), followed by incubation with broad-spectrum kinase probe XO44-Cy5 or probe WEL033 (1 µM, 30 min, rt). Protein expression was verified by immunoblot against a C-terminal V5-tag.

Quantitative label-free chemical proteomics was used to identify the off-targets of WEL028 at this concentration. The WEL028-labeled proteome was conjugated to biotin-azide post-lysis, followed by streptavidin enrichment, on-bead protein digestion and analysis of the corresponding peptides using mass spectrometry. Significantly enriched kinases in WEL028-treated samples compared to vehicle-treated samples were designated as targets (Figure 3.4A). Identified off-targets included protein kinases harboring native cysteines at the DFG-1 position (depicted in bold), as well as several metabolic kinases (ADK, PFKL, PFKP, ADPGK, NME1, PKM, PGK1), although the latter lack a DFG-motif. Notably, the off-target profile of HL-60 WT and FES^{S700C} cells was identical

with the exception of FES, which was exclusively present in mutant cells. This highlights that, despite a limited number of off-targets, WEL028 can be effectively used in comparative target validation studies between WT and FES^{S700C} HL-60 cells.

Interestingly, the identified off-targets MAPK1/3 and MAP2K1/2 are part of signaling pathways activated upon PMA treatment and are reported to be essential for HL-60 cell differentiation along the monocyte/macrophage lineage.[14] Although MAPK1 and MAPK3 were no prominent targets of WEL028 in the single-dose kinome screen at 1 µM (< 50% inhibition) (see chapter 2), both were identified as off-targets at this concentration *in situ*. This could result from different *in vitro* and *in situ* inhibitory potencies[15] or high total abundance of these kinases in cells. MAP2K1 and MAP2K2 were already identified in the *in vitro* selectivity assay and although WEL028 showed only a moderate potency on these targets (pIC_{50} = 6.6 ± 0.06), both are likely to be inhibited at a concentration of 1 µM. Accordingly, recombinantly expressed MAP2K2 was effectively visualized by fluorescent probe WEL033 *in vitro* (Figure 3.4B). Labeling was abolished upon mutagenesis of the corresponding DFG-1 cysteine into an alanine ($MAP2K2^{C211A}$), verifying that the probe has a similar covalent mode of action as on FES^{S700C}. Notably, labeling with the active site lysine-targeting probe XO44-Cy5[2] (Supplementary Scheme 3.1) and protein expression levels were similar for $MAP2K2^{WT}$ and $MAP2K2^{C211A}$. Altogether, these data suggest that the off-targets of WEL028 responsible for the observed block in differentiation at 1 µM, are likely to be members of the MAP kinase family harboring native DFG-1 cysteine residues.

CRISPR/Cas9-mediated knockout of FES does not affect PMA-induced differentiation

Although FES activity was shown to be dispensable for differentiation of HL-60 cells into macrophages, it remained unclear whether FES played a role in myeloid differentiation based on its scaffold functions. To this end, a CRISPR/Cas9 gene editing strategy was designed to disrupt the *FES* gene and entirely abrogate FES expression (Figure 3.5A). A sgRNA in exon 1 was used to induce double-strand breaks in the coding sequence, which are typically repaired via error-prone non-homologous end joining (NHEJ), generating small deletions or insertions flanking the cleavage site.[16] The use of a sgRNA in an early exon of the *FES* gene increases the probability of obtaining translational frameshifts that result in premature stop codons. Nucleofection of HL-60 cells with plasmid encoding sgRNA and Cas9 nuclease, single cell dilution and screening of clones using a T7 endonuclease I (T7E1) assay led to the identification of a FES^{KO} clone (Figure 3.5B). Decomposition of Sanger sequencing traces using the TIDE web tool[17] revealed the individual gene editing events in the two *FES* alleles, corresponding to an indel of 1 bp and an insertion of 1 bp, respectively (Figure 3.5C). Translation of the edited alleles leads to the introduction of an early stop codon and thereby results in a truncated, dysfunctional protein. In line with this analysis, no residual FES protein was detected in

HL-60 FES^{KO} lysates by immunoblot with an anti-FES antibody (Figure 3.5D). Interestingly, FES^{KO} cells also showed all characteristics of unaffected PMA-induced differentiation compared to wild-type cells, exemplified by a similar percentage of CD11b-positive cells and an identical reduction in proliferation (Figure 3.5E, F). Moreover, FES^{KO} cells acquired macrophage morphology, although cell adhesion to the plastic surface appeared to be slightly impaired (Figure 3.5G). In conclusion, not only FES activity but also FES scaffold functions appear to not be required for differentiation of HL-60 cells in response to PMA treatment.

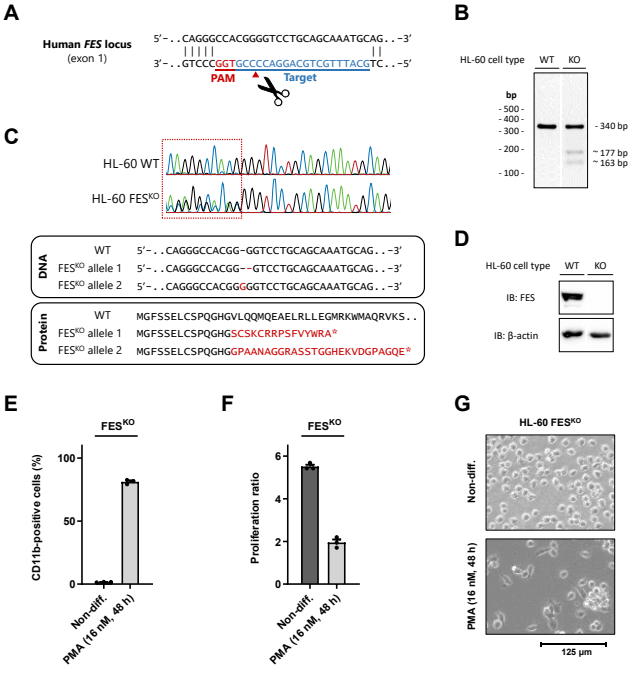

Figure 3.5 - CRISPR/Cas9-mediated knockout of FES does not affect PMA-induced differentiation. **(A)** CRISPR/Cas9 gene editing strategy for FES knockout in HL-60 cells. Selected sgRNA (bold blue) directs Cas9 to cleave at predicted site (red triangle). Repair of the induced double-strand break by non-homologous end-joining (NHEJ) results in deletions or insertions that can lead to a translational frameshift and introduction of a premature stop codon. PAM: protospacer-adjacent motif. **(B)** T7 endonuclease I (T7E1) assay for identification of HL-60 FES^{KO} clone. Genomic region was amplified by PCR and amplicons were analyzed using T7E1 assay. Expected fragment size indicating gene editing events: ~177 and ~163 bp. **(C)** Sequencing traces of WT HL-60 cells and homozygous FES^{KO} HL-60 clone. Double traces indicate different gene editing events in the two independent *FES* alleles and were decomposed using TIDE analysis (https://tide.deskgen.com). **(D)** Validation of FES knockout by immunoblot analysis on WT or FES^{KO} HL-60 cell lysate using anti-FES antibody. **(E)** CD11b surface expression of FES^{KO} HL-60 cells incubated without or with PMA (16 nM, 48 h), analyzed by flow cytometry. **(F)** Proliferation of FES^{KO} HL-60 cells incubated as in E. Proliferation ratio: live cell number after differentiation divided by live cell number before differentiation. **(G)** Morphological inspection of FES^{KO} HL-60 cells. Shown images are representative for multiple acquired images at 20x magnification from replicates. All data represent means ± SEM (N = 3). Statistical analysis was performed using ANOVA with Holm-Sidak's multiple comparisons correction, *** P <0.001; NS if P >0.05.

Discussion and conclusion

Previously reported chemical genetic methods rely on overexpression systems that disturb signal transduction cascades.[3] In contrast, a major benefit of the strategy described in this chapter lies in the ability to exert unprecedented control over a biological system without disturbing cellular homeostasis. One single atom out of 13.171 atoms in FES was replaced by changing only one base pair out of over 3.000.000.000 base pairs in the human genome. Arguably, this minimal change at the genome and protein level ensures that its regulation at transcriptional and (post-)translational level are minimally disturbed. In fact, it was demonstrated that wild-type and mutant cells behaved similarly in various functional assays (*e.g.* proliferation, differentiation, morphology and CD11b surface expression). This is in line with the comprehensive biochemical profiling of FES^{S700C} as described in chapter 2, which showed that its kinase activity, substrate preference and protein-protein interactions were similar to FES^{WT}. Yet, the conversion of an oxygen atom in a sulphur atom in the endogenously expressed protein allowed the rational design and synthesis of a chemical probe that visualizes and inhibits the engineered kinase activity in human cells.

The use of fluorescent probe WEL033 was key to visualize target engagement of FES during myeloid differentiation of HL-60 cells towards monocytes/macrophages. In contrast to previous studies relying on transient overexpression of FES or RNA knockdown approaches[7,13], no defects in differentiation were observed despite complete acute inhibition of FES activity. In line with these results, FES knockout mice display no defects in myeloid cell differentiation and survival, as reflected by unaltered numbers of various blood cell types, including monocytes and neutrophils, compared to wild-type mice[9,18]. Altogether, this study suggests that FES kinase activity is dispensable for differentiation of HL-60 cells along the monocyte/macrophage lineage. In addition, CRISPR/Cas9-mediated knockout of FES did not affect PMA-induced differentiation either, although it should be taken into account that long-term genetic disruption may lead to compensatory effects.

A major advantage of the used chemical genetic method is the ability to use wild-type cells as a control to account for potential off-target effects. In this way, even a chemical probe with a limited number of defined off-targets can be effectively used for functional studies. Indeed, the off-target profile of WEL028 was identical in both wild-type and mutant HL-60 cells and the only difference in their WEL028-reactive proteome was the engineered kinase FES. The importance of distinguishing on-target from off-target effects is illustrated by the observation that WEL028 at higher concentrations disrupted differentiation of HL-60 cells. The here presented strategy was instrumental to identify that the observed effects, however, also occurred in wild-type control cells and can thus be attributed to inhibition of off-targets, rather than FES. A competitive

chemical proteomics experiment with a broad-spectrum kinase probe, such as XO44, could be employed to quantify cellular target engagement of WEL028 on off-targets.

An interesting next step would be to explore the effect of FES inactivation during differentiation of more physiologically relevant precursor cells, such as hematopoietic stem cells (HSCs). Myeloid differentiation of these cells is induced by (complex mixtures of) growth factors and cytokines and thus relies on multiple downstream signaling pathways.[19] FES is currently under consideration as a therapeutic target for acute myeloid leukemia (AML)[20,21], a disease characterized by defective differentiation and excessive proliferation of HSCs.[22] Consequently, differentiation therapy (*e.g.* with all-*trans* retinoic acid) is currently used in some AML subtypes.[23] Further investigation of the role of FES in HSCs differentiation is thus relevant, because if FES is required for this process, FES inhibitors may possibly counter-act these AML treatments. Tremendous advancements in CRISPR/Cas9 gene editing and base editing technologies will provide means to efficiently introduce the S700C mutation in the *FES* locus in HSCs[24] and apply this chemical genetic toolbox in a more physiologically relevant model system.

Acknowledgments

Hans den Dulk is kindly acknowledged for technical assistance with cell culture, Bogdan I. Florea for mass spectrometry analysis, Rolf Boot for useful advice and providing plasmids, and Laura de Paus for synthesis of XO44-Cy5.

Experimental procedures

General

All chemicals were purchased at Sigma Aldrich, unless stated otherwise. DNA oligos were purchased at Sigma Aldrich or Integrated DNA Technologies. Cloning reagents were obtained from Thermo Fisher. XO44-Cy5 was previously synthesized in-house based on literature procedures[2] and characterized by NMR and LC-MS. All cell culture disposables were purchased at Sarstedt. Mammalian protease inhibitor cocktails were obtained from Amresco.

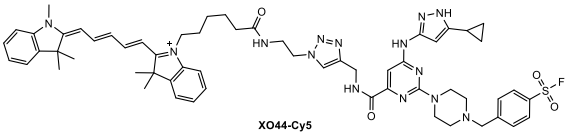

Supplementary Scheme 3.1 – Structure of active site lysine-targeting broad-spectrum kinase probe XO44-Cy5.

Cloning

For CRISPR/Cas9 plasmids, guides were cloned into the BbsI restriction site of plasmid px330-U6-Chimeric_BB-CBh-hSpCas9 (gift from Feng Zhang, Addgene plasmid #42230) as previously described.[25,26] pDONR223-construct with full-length human cDNA of MAP2K2 was a gift from William Hahn & David Root (Addgene Human Kinase ORF Collection). Eukaryotic expression constructs of MAP2K2 was generated using Gateway™ recombinational cloning into a pcDest40 vector, in frame with a C-terminal V5-tag, according to recommended procedures (Thermo Fisher). Point mutations were introduced by site-directed mutagenesis and all plasmids were isolated from transformed XL10-Gold competent cells (prepared using *E. coli* transformation buffer set; Zymo Research) using plasmid isolation kits following the supplier's protocol (Qiagen). All sequences were verified by Sanger sequencing (Macrogen).

Supplementary Table 3.3 – List of oligonucleotide sequences.

ID	Name	Sequence
P1	sgRNA_hFES-MUT_S700C_top	CACCTGACTTTGGGATGTCCCGAG
P2	sgRNA_hFES-MUT_S700C_bott	AAACCTCGGGACATCCCAAAGTCA
P3	gPCR_hFES_S700C_forw	TTTTGTCCTTGGCTTTCCTAGA
P4	gPCR_hFES_S700C_rev	GTGCTTACCCTTCTCCACAAAC
P5	HDR-template_hFES_S700C	ACTGTTGGCCAAATGAGCCCCTGCCCTGTCTCACCCAGGGACCTGGCTG CTCGGAACTGCCTGGTGACAGAGAAGAAGAATGTGCTGAAGATCTGTGACTTT GGCATGTCCCGAGAAGAAGCCGATGGGGTCTATGCAGCCTCAGGGGGC CTCAGACAAGTCCCCGTGAAGTGGACCGCACCTGAGGCCCTTAACTA
P6	sgRNA_hFES-KO_exon1_top	CACCGCATTTGCTGCAGGACCCCG
P7	sgRNA_hFES-KO_exon1_bott	AAACCGGGGTCCTGCAGCAAATGC
P8	gPCR_hFES-KO_exon1_forw	CAGTCCATCCTGACCCTACAGT
P9	gPCR_hFES-KO_exon1_rev	AGAGTCCCATAGAGACCCACCT
P10	gPCR_TTC16_forw	AGAACAGACGGTGTTGTAAGCAT
P11	gPCR_TTC16_rev	ATTAGACAGTTGAGTTCACTGAGGC
P12	gPCR_TCIRG1_forw	AGAGTCTCGTAGCTGTGTCCTTCT
P13	gPCR_TCIRG1_rev	CAGGTACACGGCCTTCATCT
P14	MAP2K2_C211A_forw	AGGGGAGATCAAGCTAGCTGACTTCGGGGTGAG
P15	MAP2K2_C211A_rev	CTCACCCCGAAGTCAGCTAGCTTGATCTCCCCT

Cell culture

General cell culture

Cell lines were purchased at ATCC and were tested on regular basis for mycoplasma contamination. Cultures were discarded after 2-3 months of use. U2OS (human osteosarcoma) cells were cultured at 37 °C under 7% CO_2 in DMEM containing phenol red, stable glutamine, 10% (v/v) heat-inactivated newborn calf serum (Seradigm), penicillin and streptomycin (200 µg/mL each; Duchefa). Medium

was refreshed every 2-3 days and cells were passaged two times a week at 80-90% confluence. HL-60 (human promyeloblast) cells were cultured at 37 °C under 5% CO_2 in HEPES-supplemented RPMI containing phenol red, stable glutamine, 10% (v/v) fetal calf serum (Biowest), penicillin and streptomycin (200 µg/mL each), unless stated otherwise. Cell density was maintained between 0.2 x 10^6 and 2.0 x 10^6 cells/mL. Cell viability was assessed by Trypan Blue exclusion and quantification using a TC20™ Automated Cell Counter (Bio-Rad).

Transfection of U2OS cells

One day prior to transfection, U2OS cells were transferred from confluent 10 cm dishes to 15 cm dishes. Before transfection, medium was refreshed (13 mL). A 3:1 (m/m) mixture of polyethyleneimine (PEI; 60 µg/dish) and plasmid DNA (20 µg/dish) was prepared in serum-free medium and incubated for 15 min at rt. The mixture was then dropwisely added to the cells, after which the cells were grown to confluence in 72 h. Cells were then harvested by suspension in PBS, followed by centrifugation for 5 min at 200 *g*. Cell pellets were flash-frozen in liquid nitrogen and stored at -80 °C until sample preparation.

Transfection of HL-60 cells

Transfection of CRISPR plasmid DNA and ssODN repair template into HL-60 cells was performed using Amaxa nucleofector kit V and nucleofector I device (Lonza). One day prior to transfection, HL-60 cells were diluted to a density of 0.4 x 10^6 cells/mL. The next day, 2 x 10^6 cells per condition were centrifuged (200 *g*, 5 min) and resuspended in 100 µL nucleofection solution. Plasmid DNA (2 µg) and if applicable ssODN repair template (400 pmol) were added and cells were nucleofected using program T-019. Cells were allowed to recover (10 min, rt) before transfer to 12-well plates in antibiotics-free medium at 37 °C.

Differentiation of HL-60 cells towards monocytes/macrophages

One day prior to induction of differentiation, cells were diluted to 0.4 x 10^6 cells/mL. The next day, monocytic/macrophage differentiation was induced by addition of phorbol 12-myristate 13-acetate (PMA) to a final concentration of 16 nM. Cells were grown for 48 h unless indicated otherwise, during which cells attached to the plastic surface and acquired macrophage characteristics. For morphological inspection, images were taken on an EVOS FL Auto 2 Imaging System (Thermo Fisher) at 20x magnification.

Inhibitor treatment in live cells

The term *in situ* is used to designate experiments in which live cell cultures are treated with inhibitor, whereas the term *in vitro* refers to experiments in which the inhibitor is incubated with cell lysates. Compounds were diluted in growth medium from a 1000x concentrated stock solution in DMSO.

For *in situ* treatment of HL-60 cells during differentiation, HL-60 cells were prepared for differentiation as described above. Cells were pre-incubated with compound for 1 h before differentiation was induced by addition of differentiation agents as described above. Medium was refreshed every 24 h with medium containing equal inhibitor and differentiation agent concentrations.

For *in situ* treatment post-differentiation, HL-60 cells were differentiated as described above, after which cells were incubated with compound for 1 h. Cells were collected by suspension for non-adherent cells and trypsinization for adherent cells. After collection, cells were centrifuged (200 *g*, 5 min, rt) and washed in equal volume of PBS (1000 *g*, 5 min, rt). Cell pellets were flash-frozen in liquid nitrogen and stored at -80 °C until use.

CRISPR/Cas9 gene editing

sgRNA selection and ssODN homology-directed repair (HDR) donor design

Selection of sgRNA was based on proximity to desired site of cleavage or mutagenesis as well as efficiency and specificity as predicted by CHOPCHOP v2 online web tool (http://chopchop.cbu.uib.no)[27]. sgRNA sequences can be found in Supplementary Table 3.3. For FES knockout, a sgRNA targeting exon 1 was selected. For FES mutagenesis, a sgRNA targeting exon 16 was selected and an ssODN HDR donor was designed that after successful HDR incorporates the desired S700C mutation along with a BglII restriction site to facilitate analysis by RFLP. Furthermore, silent mutations are incorporated to remove "NGG" protospacer adjacent motifs (PAMs), preventing recleavage of the genomic sequence after successful HDR or cleavage of the ssODN donor itself.

Single cell isolation and expansion

For preparation of conditioned RPMI medium, HL-60 cells were diluted to 0.2 x 10^6 cells/mL and grown for 48 h at 37 °C. Cell suspension was then centrifuged (1,000 *g*, 5 min) and medium was transferred to a sterile tube, followed by a second centrifugation step (3,500 *g*, 10 min). The medium was subsequently filtered through a 0.2 µm sterile filter and stored at -80 °C until use, for no longer than 3 months.

Single cell cultures were obtained approximately 7 days post-nucleofection by dilution in 1:1 conditioned and fresh RPMI medium and expanded in 96-well plates (100 µL per well). After 14 days, plates were inspected for cell growth, clones were collected in new plates and half of the volume was transferred to 96-well PCR-plates, followed by centrifugation (1,000 *g*, 10 min). Medium was removed and cell pellets were suspended in 25 µL QuickExtract™ (Epicentre). The samples were incubated at 65 °C for 6 min, mixed by vortexing and then incubated at 98 °C for 2 min. Genomic DNA extracts were diluted in sterile water and directly used in PCR reactions. Genomic PCR reactions were performed on 5 µL isolated genomic DNA extract using Phusion High-Fidelity DNA Polymerase (Thermo Fisher) in Phusion HF buffer in a final volume of 20 µL.

Genotyping assays

For T7E1 assays, genomic PCR products were mixed in a 1:1 ratio with wild-type amplicons and denatured and reannealed in a thermocycler using the following program: 5 min at 95 °C, 95 to 85 °C using a ramp rate of -2 °C/s, 85 to 25 °C using a ramp rate of -0.2 °C/s. To annealed PCR product (8.5 µL), NEB2 buffer (1 µL) and T7 endonuclease I (5 U, 0.5 µL; New England Biolabs) were added, followed by incubation at 37 °C for 30 min. Restriction Fragment Length Polymorphism (RFLP) assays were performed by directly combining genomic PCR product (8.5 µL) with FastDigest buffer (1 µL) and FastDigest BglII (0.5 µL), followed by incubation at 37 °C for 30 min. Digested PCR products were analyzed using agarose gel electrophoresis with ethidium bromide staining.

Sanger sequencing for gene editing and off-target analysis

Genomic PCR products were purified using NucleoSpin® Gel and PCR Clean-up kit (Macherey-Nagel) prior to Sanger sequencing. For knockouts, sequence traces were decomposed using the TIDE web tool (https://deskgen.com).[17] Potential off-target cleavage sites of the used sgRNA were predicted using DESKGEN™ online web tool (https://deskgen.com). Top-ranked potential coding off-target sequences containing 3 or less mismatches to the employed sgRNA sequence were selected for validation. The genomic region surrounding the potential off-target site was amplified by PCR and analyzed by Sanger sequencing.

Preparation of cell lysates

Pellets were thawed on ice and suspended in lysis buffer (50 mM HEPES pH 7.2, 150 mM NaCl, 1 mM $MgCl_2$, 0.1% (w/v) Triton X-100, 2 mM Na_3VO_4, 20 mM NaF, 1 x mammalian protease inhibitor cocktail, 25 U/mL benzonase). Cells were lysed by sonication on ice (15 cycles of 4'' on, 9.9'' off at 25% maximum amplitude). Alternatively (Figure S2-4), pellets were thawed on ice and suspended in

M-PER buffer supplemented with 1x Halt™ phosphatase and protease inhibitor cocktail (Thermo Fisher), followed by centrifugation (14,000 *g*, 10 min, 4 °C). Protein concentration was determined using Quick Start™ Bradford Protein Assay (Bio-Rad) and lysates were aliquoted, flash-frozen and stored at -80 °C until use.

Probe labeling experiments

For *in vitro* inhibition experiments, cell lysate (14 µL) was pre-incubated with inhibitor (0.5 µL, 29 x concentrated stock in DMSO, 30 min, rt), followed by incubation with probe WEL033 or XO44-Cy5 (0.5 µL, 30 x concentrated stock in DMSO, 30 min, rt). For *in situ* inhibition experiments, treated cell lysate (14.5 µL) was directly incubated with probe (0.5 µL, 30 x concentrated stock in DMSO, 30 min, rt). Final concentrations of inhibitors and/or probe are indicated in figure legends. Reactions were quenched with 4x Laemmli buffer (5 µL, final concentrations 60 mM Tris pH 6.8, 2% (w/v) SDS, 10% (v/v) glycerol, 5% (v/v) β-mercaptoethanol, 0.01% (v/v) bromophenol blue) and boiled for 5 min at 95 °C. Samples were resolved by SDS-PAGE on a 10% polyacrylamide gel (180 V, 75 min). Gels were scanned using Cy3 and Cy5 multichannel settings (605/50 and 695/55 filters, respectively; ChemiDoc™ MP System, Bio-Rad). Fluorescence intensity was corrected for protein loading determined by Coomassie Brilliant Blue R-250 staining and quantified with Image Lab (Bio-Rad). IC_{50} curves were fitted with Graphpad Prism® 7 (Graphpad Software Inc.).

Proteomics

Proteomics was performed based on previously described procedures.[28] In summary, full cell lysates of FES^{WT} and FES^{S700C} HL-60 cells incubated *in situ* with vehicle, 100 nM or 1 µM WEL028 during PMA-induced differentiation were prepared as aforementioned. Click mix was freshly prepared by combining $CuSO_4$ (1 µL of 15 mM stock), sodium ascorbate (0.6 µL of 150 mM stock), THPTA (0.2 µL of 15 mM stock) and biotin-azide (0.2 µL of 4 mM stock in DMSO). Lysates (250 µL of 2 mg/mL) were conjugated to biotin-azide using click chemistry (25 µL click mix, 1 h, 37 °C). The reaction was quenched and excess biotin-azide was removed by chloroform/methanol precipitation. Precipitated proteome was suspended in 6 M urea in 25 mM ammonium bicarbonate, reduced (10 mM DTT, 15 min, 65 °C) and alkylated (40 mM iodoacetamide, 30 min, rt, in the dark). SDS was added (2% final concentration, 5 min, 65 °C), samples were diluted in PBS and incubated with avidin beads (from 50% slurry, 3 h, rt, in overhead rotator). Beads were washed with 0.5% SDS in PBS, followed by 3 washes with PBS, and then transferred to low-binding Eppendorf tubes. Proteins were digested with trypsin overnight at 37 °C and resulting peptides were desalted using stage tips with C_{18} material. Samples were analyzed on an LC-IMS-MS system with a Synapt G2-Si instrument (Waters) as previously described [28]. Data processing was performed with ISOQuant software as previously described.[29,30] The following cut-offs were used for target identification: unique peptides ≥ 1, identified peptides ≥ 2, ratio WEL028-treated over vehicle-treated ≥ 2 with q-value <0.05 based on *t*-test with Benjamini-Hochberg multiple comparison correction (FDR = 10%), kinase annotation in Uniprot database.

Immunoblot

Samples were resolved by SDS-PAGE as described above, but transferred to 0.2 µm polyvinylidene difluoride membranes by Trans-Blot Turbo™ Transfer system (Bio-Rad) directly after fluorescence scanning. Membranes were washed with TBS (50 mM Tris pH 7.5, 150 mM NaCl) and blocked with 5% milk in TBS-T (50 mM Tris pH 7.5, 150 mM NaCl, 0.05% Tween-20) for 1 h at rt. Membranes were then either incubated with primary antibody in 5% milk in TBS-T (V5; o/n at 4 °C) or washed three times with TBS-T, followed by incubation with primary antibody in 5% BSA in TBS-T (FES, Lamin B, β-actin, o/n at 4 °C). Membranes were washed three times with TBS-T, incubated with matching secondary antibody in 5% milk in TBS-T (1 h at rt) and then washed three times with TBS-T and once with TBS. Luminol development solution (10 mL of 1.4 mM luminol in 100 mM Tris pH 8.8 + 100 µL of 6.7 mM *p*-coumaric acid in DMSO + 3 µL of 30% (v/v) H_2O_2) was added and chemiluminescence was detected on ChemiDoc™ MP System.

Primary antibodies: monoclonal rabbit anti-FES (1:1000, Cell Signaling Technology (CST), #85704), polyclonal rabbit anti-Lamin B1 (1:5000, Thermo Fisher, PA5-19468), monoclonal mouse anti-β-actin (1:1000, Abcam, ab8227), monoclonal mouse anti-V5 (1:5000, Thermo Fisher, R960-25). Secondary antibodies: goat anti-mouse-HRP (1:5000, Santa Cruz, sc-2005), goat anti-rabbit-HRP (1:5000, Santa Cruz, sc-2030).

CD11b expression analysis by flow cytometry

Cells ($1x10^6$ per sample) were centrifuged (500 *g*, 3 min) and suspended in human FcR blocking solution (Miltenyi Biotec, 25x diluted in FACS buffer (1% BSA, 1% FCS, 0.1% NaN_3, 2 mM EDTA in PBS)), transferred to a V-bottom 96-well plate and incubated for 10 min at 4 °C. Next, monoclonal rat CD11b-APC antibody (1:100, Miltenyi Biotec, 130-113-231) or rat anti-IgG2b-APC isotype control antibody (1:100, Miltenyi Biotec, 130-106-728) was added along with 7-AAD (7-aminoactinomycin D; 1 µg/mL) and samples were incubated for 30 min 4 °C in the dark. Samples were washed once in PBS and fixed in 1% PFA in PBS for 15 min at 4 °C in the dark, followed by two washing steps in PBS and resuspension in FACS buffer to a density of approximately 500 cells/µL. Cell suspensions were measured on a Guava easyCyte HT and data was processed using GuavaSoft InCyte 3.3 (Merck Millipore). Events (generally 10,000 per condition) were gated by forward and side scatter (cells), side scatter area (singlets) and viability (live cells) and the percentage of CD11b-positive cells was determined based on background fluorescence for isotype control antibody and non-differentiated cells. The RED-R channel (661/15 filter) and RED-B channel (695/50 filter) were used to detect CD11b-APC and 7-AAD, respectively.

Statistical analysis

All statistical measures and methods are included in the respective Figure or Table captions. In brief: all replicates represent biological replicates and all data represent means ± SEM, unless indicated otherwise. Statistical significance was determined using Student's *t*-tests (two-tailed, unpaired) or ANOVA with Holm-Sidak's multiple comparisons correction. *** $P < 0.001$; ** $P < 0.01$; * $P < 0.05$; NS if $P > 0.05$. All statistical analyses were conducted using GraphPad Prism® 7 or Microsoft Excel.

Supplementary Data

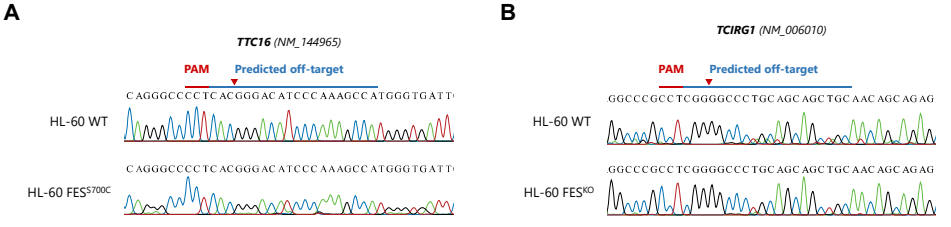

Supplementary Figure 3.1 - Analysis of putative sgRNA off-target sites. (A, B) Analysis of the only predicted coding off-targets of the sgRNA target sequence employed for FES^{S700C} mutagenesis, located in the *TTC16* gene (A), or for FES knockout, located in the *TCIRG1* gene (B). Genomic region surrounding putative off-target site was amplified by PCR, followed by Sanger sequencing analysis. No off-target gene editing events were observed.

Supplementary Table 3.1 - List of putative off-target cleavage sites for sgRNA employed in CRISPR/Cas9-mediated mutagenesis of FES. Specificity of sgRNA was assessed using DESKGEN™ online web tool (www.deskgen.com). Sites with 3 or less mismatches compared to the sgRNA target were included. Only 1 putative off-target is located in the coding region of a gene.

S700C

Mismatches	0	1	2	3
Coding	0	0	**1**	0
Non-coding	0	0	1	12

Potential off-target sequence	PAM	Similarity	Mismatches	Gene	Locus
TGGCTTTGGGATGTCCCGTG	**AGG**	**5**	**3,19**	**Yes**	**chr9@ 127716868-127716891**
TGACTTTGGCATGTCCTGAG	AGG	3	10,17	No	chr16@ 50371486-50371509
TTAGTTTGGGATGTCCAGAG	GGG	1	2,4,17	No	chr2@ 147874374-147874397
TGCCTTTGGTATGTCCAGAG	TAG	1	3,10,17	No	chr13@ 25630797-25630820
AGACTTTGGGAGGTCCCGTG	CAG	1	1,12,19	No	chr12@ 11447626-11447649
TGGCTGTGGGATGTCCCCAG	GAG	0	3,6,18	No	chr3@ 13295903-13295926
TGAGTCTGGGATGTCCCTAG	AGG	0	4,6,18	No	chr5@ 137202156-137202179
TGGCTTTGGGATGTCGGGAG	AAG	0	3,16,17	No	chr20@ 61773235-61773258
TGAATTTGGGATGTCCCATG	TAG	0	4,18,19	No	chr5@ 135589616-135589639
TGAATTTGGGATGCCCTGAG	AGG	0	4,14,17	No	chr5@ 61639561-61639584
TGACGTTGGGATGACCAGAG	CAG	0	5,14,17	No	chr19@ 35077359-35077382
TGACTTTGGGTTGTCCCCAT	GAG	0	11,18,20	No	chrX@ 112142232-112142255
TGACTTTGGGGTCTCCCAAG	AGG	0	11,13,18	No	chr2@ 95278649-95278672

Supplementary Table 3.2 - List of putative off-target cleavage sites for sgRNA employed in CRISPR/Cas9-mediated knockout of FES. Specificity of sgRNA was assessed using DESKGEN™ online web tool (www.deskgen.com). Sites with 3 or less mismatches compared to the sgRNA target were included. Only 1 putative off-target is located in the coding region of a gene.

KO

Mismatches	0	1	2	3
Coding	0	0	0	**1**
Non-coding	0	0	1	23

Potential off-target sequence	PAM	Similarity	Mismatches	Gene	Locus
GCAGCTGCTGCAGGGCCCCG	**AGG**	**1**	**4,5,15**	**Yes**	**chr11@ 68043858-68043881**
GCATTTGATGCAGGACCCCT	CAG	4	8,20	No	chr10@ 123647319-123647342
GGCTTTGCTCCAGGACCCCG	AGG	2	2,3,10	No	chr15@ 73308252-73308275
GCAGTTACTCCAGGACCCCG	AAG	2	4,7,10	No	chr11@ 124673324-124673347
GCCCTTGCTGCAGGACCCCC	AAG	1	3,4,20	No	chr17@ 40461935-40461958
GCAGCTGCTGCAGGACCCCT	GAG	1	4,5,20	No	chr15@ 88681640-88681663
AGATTTGCTGCAGGACCCTG	AAG	1	1,2,19	No	chr10@ 127843251-127843274
GCATTTACTTCTGGACCCCG	GGG	1	7,10,12	No	chr10@ 119366165-119366188
CCATTTGCTGCTGGACCCCA	GAG	1	1,12,20	No	chr17@ 49938799-49938822
GCACTTCCTGCAGGACCCTG	GGG	1	4,7,19	No	chr11@ 1161797-1161820
GCAATTACTGCAGGACCCAG	CAG	1	4,7,19	No	chr3@ 14607567-14607590
GCAGTTGCTGCTGGACCCAG	GGG	1	4,12,19	No	chr10@ 117925154-117925177
GGATTTGCTGCAGGACTCTG	GAG	0	2,17,19	No	chr19@ 58096538-58096561
GCACTTGCTGCAGGACTCTG	CAG	0	4,17,19	No	chr4@ 173717653-173717676
ACATTTGCTGCAGGCCCCAG	AGG	0	1,15,19	No	chr5@ 144567565-144567588
GGATTTGCTGCAGGTCCCTG	CAG	0	2,15,19	No	chr18@ 46311931-46311954
TCATTTGCTGCAGGAACCCT	GAG	0	1,16,20	No	chr2@ 240787656-240787679
GCATTTACTGCATGACCCTG	GGG	0	7,13,19	No	chr16@ 59837242-59837265
GCATTTACTGCAGGACTCAG	GGG	0	7,17,19	No	chr14@ 98430008-98430031
GCATTTGCTGGAGGACTCCA	GAG	0	11,17,20	No	chr14@ 64605317-64605340
GCATTCGCTGCAGGACTCTG	CAG	0	6,17,19	No	chr6@ 32495339-32495362
GCATTTGCAGCAGGTCCCAG	GAG	0	9,15,19	No	chr20@ 63162513-63162536
GCATTTGCTGCCGGAGCCCC	AAG	0	12,16,20	No	chr16@ 1264116-1264139

References

1. Jordan, J. D., Landau, E. M. & Iyengar, R. Signaling Networks. *Cell* **103**, 193–200 (2000).
2. Zhao, Q. *et al.* Broad-spectrum kinase profiling in live cells with lysine-targeted sulfonyl fluoride probes. *J. Am. Chem. Soc.* **139**, 680–685 (2017).
3. Prelich, G. Gene overexpression: Uses, mechanisms, and interpretation. *Genetics* **190**, 841–854 (2012).
4. Haigh, J., McVeigh, J. & Greer, P. The fps/fes tyrosine kinase is expressed in myeloid, vascular endothelial, epithelial, and neuronal cells and is localized in the trans-golgi network. *Cell growth Differ.* **7**, 931–44 (1996).
5. Yu, G., Smithgall, T. E. & Glazer, R. I. K562 leukemia cells transfected with the human c-fes gene acquire the ability to undergo myeloid differentiation. *J. Biol. Chem.* **264**, 10276–10281 (1989).
6. Kim, J. & Feldman, R. A. Activated Fes protein tyrosine kinase induces terminal macrophage differentiation of myeloid progenitors (U937 cells) and activation of the transcription factor PU.1. *Mol. Cell. Biol.* **22**, 1903–18 (2002).
7. Manfredini, R. *et al.* Antisense inhibition of c-fes proto-oncogene blocks PMA-induced macrophage differentiation in HL60 and in FDC-P1/MAC-11 cells. *Blood* **89**, 135–145 (1997).
8. Hackenmiller, R., Kim, J., Feldman, R. A. & Simon, M. C. Abnormal stat activation, hematopoietic homeostasis, and innate immunity in c-fes(-/-) mice. *Immunity* **13**, 397–407 (2000).
9. Senis, Y. *et al.* Targeted disruption of the murine fps/fes proto-oncogene reveals that Fps/Fes kinase activity is dispensable for hematopoiesis. *Mol. Cell. Biol.* **19**, 7436–7446 (1999).
10. Greer, P. Closing in on the biological functions of Fps/Fes and Fer. *Nat. Rev. Mol. Cell Biol.* **3**, 278–89 (2002).
11. Birnie, G. D. The HL60 cell line: a model system for studying human myeloid cell differentiation. *Br. J. Cancer* **9**, 41–45 (1988).
12. Hauert, A. B., Martinelli, S., Marone, C. & Niggli, V. Differentiated HL-60 cells are a valid model system for the analysis of human neutrophil migration and chemotaxis. *Int. J. Biochem. Cell Biol.* **34**, 838–854 (2002).
13. Kim, J., Ogata, Y., Ali, H. & Feldman, R. a. The Fes tyrosine kinase: a signal transducer that regulates myeloid-specific gene expression through transcriptional activation. *Blood Cells. Mol. Dis.* **32**, 302–308 (2004).
14. Miranda, M. B., McGuire, T. F. & Johnson, D. E. Importance of MEK-1/-2 signaling in monocytic and granulocytic differentiation of myeloid cell lines. *Leukemia* **16**, 683–92 (2002).
15. van Esbroeck, A. C. M. *et al.* Activity-based protein profiling reveals off-target proteins of the FAAH inhibitor BIA 10-2474. *Science* **356**, 1084–1087 (2017).
16. Maruyama, T. *et al.* Increasing the efficiency of precise genome editing with CRISPR-Cas9 by inhibition of nonhomologous end joining. *Nat. Biotechnol.* **33**, 538–42 (2015).
17. Brinkman, E. K., Chen, T., Amendola, M. & Van Steensel, B. Easy quantitative assessment of genome editing by sequence trace decomposition. *Nucleic Acids Res.* **42**, e168–e168 (2014).
18. Zirngibl, R. A., Senis, Y. & Greer, P. A. Enhanced Endotoxin Sensitivity in Fps/Fes-Null Mice with Minimal Defects in Hematopoietic Homeostasis. *Mol. Cell. Biol.* **22**, 2472–2486 (2002).
19. Wahlster, L. & Daley, G. Q. Progress towards generation of human haematopoietic stem cells. *Nature Cell Biology* **18**, 1111–1117 (2016).
20. Voisset, E. *et al.* FES kinases are required for oncogenic FLT3 signaling. *Leukemia* **24**, 721–728 (2010).
21. Weir, M. C. *et al.* Dual inhibition of Fes and Flt3 tyrosine kinases potently inhibits Flt3-ITD+ AML cell growth. *PLoS One* **12**, e0181178 (2017).
22. Arber, D. A. Acute Myeloid Leukemia. *N. Engl. J. Med.* **373**, 1136–1152 (2015).
23. Degos, L. & Wang, Z. Y. All trans retinoic acid in acute promyelocytic leukemia. *Oncogene* **17**, 7140–7145 (2001).
24. Bak, R. O., Dever, D. P. & Porteus, M. H. CRISPR/Cas9 genome editing in human hematopoietic stem cells. *Nat. Protoc.* **13**, 358–376 (2018).
25. Cong, L. *et al.* Multiplex Genome Engineering Using CRISPR/Cas System. *Science (80-.).* **339**, 819–824 (2013).
26. Ran, F. A. *et al.* Genome engineering using the CRISPR-Cas9 system. *Nat. Protoc.* **8**, 2281–2308 (2013).
27. Labun, K., Montague, T. G., Gagnon, J. A., Thyme, S. B. & Valen, E. CHOPCHOP v2: a web tool for the next generation of CRISPR genome engineering. *Nucleic Acids Res.* **44**, 272–276 (2016).
28. Van Rooden, E. J. *et al.* Mapping in vivo target interaction profiles of covalent inhibitors using chemical proteomics with label-free quantification. *Nat. Protoc.* **13**, 752–767 (2018).
29. Kuharev, J., Navarro, P., Distler, U., Jahn, O. & Tenzer, S. In-depth evaluation of software tools for data-independent acquisition based label-free quantification. *Proteomics* **15**, 3140–3151 (2015).
30. Distler, U., Kuharev, J., Navarro, P. & Tenzer, S. Label-free quantification in ion mobility-enhanced data-independent acquisition proteomics. *Nat. Protoc.* **11**, 795–812 (2016).